Rotator and melting transition in paraffins

A. Holz, J. Naghizadeh, and D. T. Vigren
Fachrichtung Theoretische Physik, Universität des Saarlandes, 66 Saarbrücken, Federal Republic of Germany
(Received 24 May 1982)

A theory of the melting of paraffins is developed based on dislocation theory. The transition from two- to three-dimensional melting behavior, when proceeding from the small- to large-chain limit, is qualitatively described by this theory. It also yields a tentative explanation of the tendency of large-chain polymer crystals to crystallize in a folded structure. The structural properties of the paraffin lamellae above the rotator transition and below the melting point are studied by considering vortex loop defects. The geometrical implications of the motion of vortex and dislocation loops on the lamellar structure is studied, and a roughening of the surfaces of the lamellae is predicted. The possibility of a nematic ordering of the melt is discussed.

I. INTRODUCTION

Paraffins crystallize in lamellar form with a layer thickness approximately equal to the extended chain length. For the series of paraffins between C_{44} and C_{100} the melting point T_m is known to be given by the simple equation[1]

$$T_m=\frac{\Delta H^*(n+a)}{\Delta S^*(n+b)}\simeq T_m^*\frac{n+a}{n+b}\ , \tag{1}$$

where ΔH^* and ΔS^* represent, respectively, the heat and entropy of melting per CH_2 unit, n the chain length, a and b the end group heat and entropy of melting. T_m^* is the asymptotic melting point as $n\rightarrow\infty$ and should correspond to the extended chain polyethylene. Flory and Vrij[2] and others[3] have presented modifications of Eq. (1). In Fig. 1, T_m is plotted against n.

The purpose of this work is to study some aspects of the melting transition (which is usually preceded by a so-called rotator transition) as a function of layer thickness, in terms of the two- and three-dimensional dislocation theory of melting.[4–6] In fact, even the short-chain problem can only be considered as quasi-two-dimensional, due to interlayer coupling. The possible transitions of such a short-chain system from smectic B to smectic A to nematic and finally to the isotropic liquid have already been studied by Hubermann *et al.*[7] using a dislocation theory. Accordingly, in this paper, emphasis is given to the thickness dependence of the phase-transition phenomena. The crucial problem is how to handle dislocations, constructed on extended objects like polymers, within a melting theory.

In the low-temperature phase of paraffin the polymers form an orthorhombic structure.[3] Here the CH_2 units of a single chain are arranged on a low-angle zig-zag structure, where the zig-zag planes of neighboring chains are orthogonal. The disordering of the zig-zag planes occurs during the rotator transition at T_r.[8] It is accompanied by an orthorhombic to hexagonal structural transition and a considerable expansion of the lattice. Although the rotator transition does not alter the system's long-range lateral hexagonal order, it seems that the layer structure becomes ill defined.[9] Obviously, the elastic constants entering the dislocation theory of melting are those of the disordered-rotator phase, and will depend on the magnitude of $(T_m-T_r)/T_r$ as well as upon the strength of the discontinuity of the rotator transition (i.e., on the short-range order of the twisted zig-zag planes of the CH_2 units which remain above T_r). Consequently, a quantitative prediction of melting temperatures will not be

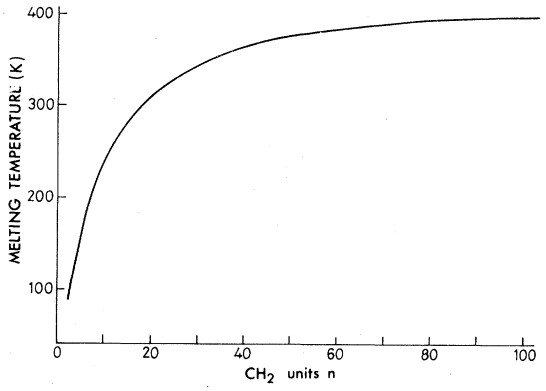

FIG. 1. Melting temperature T_m of paraffin as a function of crystal thickness, measured in CH_2 units n.

attempted, but only a qualitative theory of the polymer length dependence of T_m will be given. In addition, the geometrical implications for the polymer arrangements, arising from the presence of dislocations, and also the vortex defects which appear in the rotator phase, will be studied.

In Sec. II the melting problem is studied in a simplified model which ignores the complications arising from the rotator degrees of freedom. In Sec. III the disordered-rotator phase is treated assuming that the transition is driven by the generation of vortices. The interrelation between the rotational and translational degrees of freedom is studied in Sec. IV in connection with a possible smectic A or nematic structure of the paraffin melt. In Sec. V a discussion of the results and its shortcomings are given.

II. SIMPLIFIED TREATMENT OF PARAFFIN MELTING

We assume in this section that the paraffin layers are reasonably well defined, and that the interlayer structure is of a highly plastic, or even viscous, nature in the relevant temperature region, such that a decoupled layer approximation may be employed. The correct melting criterion of one layer can be developed by considering the asymptotic behavior of the following correlation function:

$$\langle \exp i\vec{K}\cdot(\vec{r}^{\,n}-\vec{r}^{\,m})\rangle \ , \tag{2}$$

where $\vec{K}$ is a reciprocal-lattice vector. This vector may lie either within or perpendicular to the layer plane. In the former case exponential decay of Eq. (2) marks fluid behavior with respect to shear forces in the layer plane, and in the latter case with respect to shear forces normal to the layer plane. The former melting transition is produced through dissociation of edge dislocation pairs whose Burgers vectors $\vec{b}^{||}$ lie in the plane. The latter melting transition is produced when pairs of screw dislocations with Burgers vector $\vec{b}^{\perp}$ normal to the plane dissociate. Pairs of dislocations which penetrate the lamella fully are termed "bridging loops." In this paper we will consistently denote loops as edge or screw type, according to their edge or screw character at the points where they penetrate the lamellar surfaces, even in the case where the loop begins and ends on a single surface.

It can be shown that the transition of Eq. (2) from an algebraic decay law to exponential decay can be studied by means of the renormalized coupling constants of the theory[10] (Hooke's tensor). This tensor can be obtained by means of the following series of steps. In the harmonic approximation[10] the displacement correlation function can be presented in the form

$$\langle S_{\vec{q},j}S_{-\vec{q},i}\rangle=\langle S^e_{\vec{q},j}S^e_{-\vec{q},i}\rangle+\langle p_{\vec{q},j}p_{-\vec{q},i}\rangle \ , \tag{3a}$$

where

$$S_{\vec{q},j}=S^e_{\vec{q},j}+p_{\vec{q},j} \tag{3b}$$

is a decomposition of the Fourier transformed displacement $\vec{S}_{\vec{q}}$ into elastic (S^e_q) and plastic (P_q) displacements. Employing the Einstein summation convention, we may write $P_{-\vec{q},j}$ as[10]

$$p_{-\vec{q},j}=\frac{i}{\sqrt{N}}\Phi^{-1}_{j,k}(\vec{q})\sum_{\sigma}\sum_{(\text{loop }\sigma)}\int_{\Sigma^\sigma}e^{-i\vec{q}\cdot\vec{r}^{\,\sigma}}C^e_{ks,im}b^\sigma_i q_s d^2r^\sigma_m \ , \tag{4}$$

where $C^e_{ks,im}$ is Hooke's elastic tensor (temperature renormalized, due to phonon excitations), and N is the total number of lattice units (CH_2 groups). The integral is performed over the surface Σ^σ spanned by the dislocation loop with Burgers vector $\vec{b}^\sigma$, where $\sigma=||$ or $\perp$ implies the direction parallel or perpendicular to the lamellar plane. The sum $\sum_{(\text{loop }\sigma)}$ is taken over all loops of given σ. The quantity $\Phi^{-1}(\vec{q})$ is the unperturbed propagator defined by

$$\langle S^e_{\vec{q},j}S^e_{-\vec{q},i}\rangle=2k_BT\Phi^{-1}_{j,i}(\vec{q}) \ . \tag{5}$$

Inserting Eq. (4) into Eq. (3) one obtains using Eq. (5)

$$\langle S_{\vec{q},j}S_{-\vec{q},i}\rangle=2k_BT\{\Phi^{-1}(\vec{q})[I+2\pi\chi(\vec{q})]\}_{ji} \ , \tag{6}$$

where I is the unit matrix and $\chi(\vec{q})$ is the generalized susceptibility tensor defined by

$$\chi_{k,r}(\vec{q})=\frac{1}{4\pi k_BTN}\left\langle\left[\sum_\sigma\int_{\Sigma^\sigma}e^{i\vec{q}\cdot\vec{r}^{\,\sigma}}C^e_{ks,pm}b^\sigma_p q_s d^2r^\sigma_m\right]\left[\sum_{\sigma'}\int_{\Sigma^{\sigma'}}e^{i\vec{q}\cdot\vec{r}^{\,\sigma'}}C^e_{k's',p'm'}b^{\sigma'}_{p'}q_{s'}d^2r^{\sigma'}_{m'}\right]\right\rangle\Phi^{-1}_{k',r}(\vec{q}) \ . \tag{7}$$

The thermal average is taken over the grand canonical ensemble of dislocation loops. Because the inverse propagator $\Phi_{ji}(\vec{q})$ is linearly dependent on Hooke's tensor, one needs only to invert Eq. (6) to obtain the renormalized Hooke's tensor. After some calculation we obtain

$$C^r_{is,js'} = \lim_{q\to 0}[I + 2\pi\chi(\vec{q})]^{-1}_{ik} C^e_{ks,js'} \ . \tag{8}$$

Because for short-range interacting systems $\Phi^{-1}(\vec{q}) \sim 1/q^2$, the limit in Eq. (8) exists, as can be seen from the form of Eq. (7).

In a similar way Eq. (2) can be studied[10] using the decomposition given by Eq. (3b). The transition from algebraic to exponential decay is then a consequence of the divergence of $\chi(\vec{q})$. In order to evaluate $\chi(\vec{q})$ one of several methods can be used.[5,6] Depending on the assumption as to the nature of the screened pair interaction, a continuous or discontinuous melting transition can be obtained. As this problem remains unsettled in the case of two- as well as three-dimensional systems, we will not attempt to develop a precise theory of the transition. Instead we will derive a qualitative formula for the melting temperature, based on a simple instability criterion.

Dislocation loops will be termed "closed" if they are contained fully within a single lamella. Those dislocations piercing through the surface of the lamella are considered to end there since the interlamella coupling is very weak.[8] Those loops piercing through both surfaces ("bridging loops") are most effective in screening shearing motions. Such bridging loops are most probably formed at a single interlamellar surface in the form of a small loop which begins and ends on this surface. The loop then grows through a thermally activated process until one point of the loop touches the opposite lamellar surface to form a bridging loop. Although this nucleation process may be an inherent aspect of the melting transition, in this paper it will be ignored and a finite density of bridging loops will be assumed to exist below T_m.

The evaluation of Eq. (7) for such bridging dislocation loops (for the sake of simplicity also called pairs in the following) whose core lines are more or less straight can be done approximately as follows. Equation (7) contains integrals over the surfaces Σ^σ and $\Sigma^{\sigma'}$ whose boundaries are the more or less straight dislocation lines, and the "orientation vectors" $\pm\vec{r}_\sigma$ characterize their lateral extension and orientation. Accordingly, the integral will be proportional to d^2. Furthermore, the number of lattice units N (CH_2 groups), will satisfy $N = N_p d/l$, where N_p is the number of polymers and l is the projected length of one CH_2 unit along the polymer axis. In this approximation Eq. (7) becomes

$$\chi(\vec{q}) \sim d\langle f_{\vec{q}^0}(\{\vec{r}_\sigma \cdot q_{||}, dq_\perp\}, \{\vec{r}_q\})\rangle \ , \tag{9}$$

where $\vec{q} = q\vec{q}^0 = (q_{||}, q_\perp)$ and $(||,\perp)$ signify as usual components parallel and perpendicular to the lamellar plane. The function $f_{\vec{q}^0}$ is bilinear in the $\vec{r}_\sigma$'s. Because in the derivation of Eq. (7) the boundary conditions at the lamellar surfaces on the propagator $\Phi^{-1}(\vec{q})$ have been ignored, periodic boundary conditions must be imposed normal to the lamella plane, implying $|q_\perp| \geq q_c \equiv 2\pi/d$.

For $T < T_m$, where the bridging loops consist of bound pairs, the exponential factors in Eq. (7) can be set equal to one and lead to

$$\chi(\vec{0}) \sim d\langle f_{\vec{q}^0}(\{\vec{r}_\sigma\})\rangle \ .$$

The interaction energy entering the thermal average in Eq. (9) will be calculated within the same approximation as that leading to $f_{\vec{q}^0}$; that is, periodic boundary conditions will be imposed perpendicular to the lamellar plane. It follows from this and the form of Eq. (9) that as long as we are interested in susceptibilities within the lamellar plane (i.e., $q_\perp = q_c$), the interaction energies of pairs may be expressed as

$$U^{||}_{\text{eff}}(r) = \frac{b^2_{||} K^r_{||}(r) d}{4\pi}[\ln(r/r_0) - \tfrac{1}{2}\cos 2\theta] + 2\mu^c_{||} d + 2F^k_{||}(T,d) \ , \tag{10a}$$

$$U^{\perp}_{\text{eff}}(r) = \frac{b^2_{\perp} K^r_{\perp}(r) d}{4\pi}\ln(r/r_0) + 2\mu^c_{\perp} d + 2F^k_{\perp}(T,d) \ , \tag{10b}$$

where r_0 is the dislocation core cutoff, μ^c_σ represents the core energy of a dislocation of type $\sigma(\equiv||,\perp)$, and $d \gg l$ is assumed. The first expression applies to the interaction energy between pairs of edge dislocations a distance r apart. Here $K^r_{||}(r)$ is the renormalized shear coupling constant in the plane and θ is the angle between $\vec{b}_{||}$ and the separation vector of the pair. $F^k_{||}(T,d)$ represents the free energy of the kinked dislocation core. Similarly, Eq. (10b) applies to pairs of screw dislocations. Because the two-dimensional packing is hexagonal, isotropic coupling has been assumed for shear in the layer plane as well as perpendicular to it. It should be noted that Eqs. (10a) and (10b) represent a decomposition into the elastic interaction energy plus the

conformational free energy of the dislocation line. This is only sensible as long as the "center of gravity" of each dislocation line of the pair is well defined as is suggested by the derivation of Eq. (9). This implies that Eqs. (10a) and (10b) apply to almost straight dislocation lines at any r, or for dislocation lines with a strong lateral spread and large r.

The usual instability criterion for the dissociation of a pair of type σ is[5,6]

$$\langle r_\sigma^2/r_0^2\rangle \to \infty, \quad \sigma \equiv \perp, || \ . \tag{11}$$

One immediately obtains, with the use of Eqs. (10a) and (10b)

$$k_B T_m^\sigma = \frac{b_\sigma^2 K_\sigma^r(\infty) y_\sigma}{16\pi} d \ , \tag{12}$$

where $y_\perp = 1$ and $1 \le y_{||} \le \frac{4}{3}$. For $y_{||} = 1$ it must be assumed that nonconservative motion of dislocations is easily possible, a problem which will be discussed later. The upper limit, $y_{||} = \frac{4}{3}$, corresponds to purely conservative motion.[11] For screw dislocations this problem does not arise. In order to calculate $K_\sigma^r(\infty)$ one notes that $\chi(\vec{q})$, given by Eq. (7), involves a pair-pair correlation function which for bound pairs, can be evaluated by setting the exponentials equal to 1 and letting $q \to 0$. With the use of the approximate expression given by Eq. (9) one obtains in leading order the following shear susceptibilities

$$\chi_\sigma(0) = \frac{b_\sigma^2 K_\sigma^e \alpha_\sigma d}{4\pi^2 k_B T N_p} \sum_{\sigma',\sigma''} \langle (\vec{r}_{\sigma'} \cdot \vec{\mathcal{M}})(\vec{r}_{\sigma''} \cdot \vec{\mathcal{M}}) \rangle_0 \ , \tag{13}$$

where $\vec{\mathcal{M}}$ is an arbitrary unit vector in the lamellar plane, and α_σ is a factor of order 1. This parameter is introduced to account for the separation of shear contributions to the susceptibility from the elastic constants $\{C_{is,js'}\}$, embodied in K_σ^e.[12] In Eq. (13) the subindex 0 is used to indicate that the thermal average should be taken with unrenormalized interactions.

Under the assumption that all pair-pair correlations can be neglected, only the diagonal terms of Eq. (13) contribute, and one obtains

$$\chi_\sigma(0) \simeq \frac{b_\sigma^2 K_\sigma^e \alpha_\sigma d}{8\pi^2 k_B T} n_\sigma \langle r_\sigma^2 \rangle_0 \ . \tag{13'}$$

Equation (13') neglects all higher-order effects on the susceptibility such as Lorentz field corrections, etc., and n_σ represents the density of pairs of type σ.

Using the simplified susceptibility of Eq. (13') to express the renormalized coupling constant $K_\sigma(r)$ in terms of K_σ^e in the manner of Eq. (8), Eq. (12) becomes

$$z_\sigma = \left[1 + \frac{4\alpha_\sigma}{z_\sigma y_\sigma} n_\sigma \langle r_\sigma^2 \rangle_0\right]^{-1} , \tag{12'}$$

where $z_\sigma \equiv \xi_\sigma/d$ and the reduced melting temperature ξ_σ is defined as follows:

$$\xi_\sigma \equiv \left[\frac{16\pi}{b_\sigma^2 K_\sigma^e y_\sigma}\right] k_B T_m^\sigma \ . \tag{14}$$

In the ideal gas approximation the quantity $n_\sigma \langle r_\sigma^2 \rangle_0$ may be explicitly evaluated[5] as

$$n_\sigma \langle r_\sigma^2 \rangle_0 = \frac{\pi}{2} \frac{y_\sigma z_\sigma}{1 - z_\sigma} \times \exp\{-2[\gamma_\sigma^c + f_\sigma(\xi_\sigma, d)]/z_\sigma\} \ , \tag{15}$$

where we define the dimensionless quantities

$$\gamma_\sigma \equiv 16\pi\mu_\sigma/(b_\sigma^2 K_\sigma^e y_\sigma) \tag{15a}$$

and

$$f_\sigma(\xi_\sigma, d) \equiv (\gamma_\sigma/\mu_\sigma d) F_\sigma^k(T, d) \ . \tag{15b}$$

Here γ_σ refers to the core contribution of a *straight* dislocation bridge, whereas f_σ represents the free energy of an arbitrary bridging loop with γ_σ subtracted out. Substitution of Eq. (15) into Eq. (12') yields

$$[f_\sigma(\xi_\sigma, d) + \gamma_\sigma] = -\frac{z_\sigma}{2} \ln \frac{(1 - z_\sigma)^2}{\alpha'_\sigma z_\sigma} \equiv \epsilon(z_\sigma) \ , \tag{16}$$

where $\alpha'_\sigma \equiv (\pi/2)\alpha_\sigma$. Equation (16) forms the basis of our description of the melting transition.

For short polymer chains with d less than some value d_0, the melting temperature becomes so low that the thermal excitation of kinks in the solid state cannot occur. In this "stiff polymer" limit only straight dislocation bridges are possible so that f_σ vanishes. If the renormalization of the interaction due to screening is neglected (i.e., $\alpha'_\sigma = 0$), it follows from Eq. (12') that $z_\sigma = 1$. For $\alpha_\sigma > 0$, Eq. (16) admits two solutions, one of which is greater than 1, the other, less than 1. Only the latter is physically significant since it implies a lowering of T_m^σ in the screened case as can be seen from Eqs. (12') and (14). Calling $z_\sigma^<(\alpha_\sigma)$ the solution of Eq. (16) for $d < d_0$, one obtains from Eq. (14)

$$k_B T_m^{\sigma} = \frac{b_\sigma^2 K_\sigma^e}{16\pi} y_\sigma z_\sigma^{<}(\alpha_\sigma) d, \quad d < d_0 \, . \tag{17}$$

Therefore, one obtains the expected linear dependence of T_m on the lamella thickness in the stiff polymer limit.[7] Here it should be noted that since $f_\sigma = 0$ for $d < d_0$, $z_\sigma^{<}$ is independent of d as can be seen from Eq. (16).

For $d > d_0$ it is assumed that kinks may be thermally generated in the dislocation core line, implying $f_\sigma(\xi_\sigma, d > d_0) < 0$, since conformations of the dislocation bridges must lower the free energy of the system. The qualitative behavior of $\epsilon_\sigma(z_\sigma)$ defined by Eq. (16) is sketched in Fig. 2(a). It takes the value 0 at z_σ^* given by

$$z_\sigma^* = (1+\alpha_\sigma'/2)\{1-[1-(1+\alpha_\sigma'/2)^{-2}]^{1/2}\} \tag{18}$$

and is positive in the interval $[z_\sigma^*, 1]$. Since $f_\sigma(\xi_\sigma, d > d_0) < 0$ implies that the $\epsilon_\sigma(z_\sigma)$ decreases from its value in the stiff polymer limit, and since $\epsilon_\sigma(z_\sigma)$ decreases monotonically with decreasing z_σ in the interval $[z_\sigma^*, 1]$, it follows that $z_\sigma(d) < z_\sigma^{<}$ for $d > d_0$. In view of Eq. (17) the convex behavior of T_m^{σ} as a function of d becomes apparent.

For $d \gtrsim d_0$, $|f_\sigma(\xi_\sigma, d)| \ll \gamma_\sigma$ must still hold to a good approximation and Eq. (16) takes the simplified form

$$z_\sigma / z_\sigma^0 \simeq 1 + 2\left[\frac{1-z_\sigma^0}{z_\sigma^0}\right] f_\sigma(z_\sigma^0 d, d) \, , \tag{16'}$$

where z_σ^0 is the value of z_σ for $d = d_0$. Use of Eq. (16') in Eq. (17) shows explicitly this convex behavior. For the following discussion the thermodynamic relations should be observed:

$$f_\sigma(\xi_\sigma, d) < 0, \quad \frac{\partial(f_\sigma d)}{\partial d} < 0, \quad \text{and} \quad \frac{\partial f_\sigma}{\partial \xi_\sigma} < 0 \, . \tag{19}$$

The total derivative of Eq. (16) may be written as

$$\frac{\partial f_\sigma}{\partial \xi_\sigma}\xi_\sigma' + \frac{\partial f_\sigma}{\partial d} = \tfrac{1}{2}(\xi_\sigma' d^{-1} - \xi_\sigma d^{-2}) g(z_\sigma) \, , \tag{20}$$

where

$$g(z_\sigma) \equiv -\ln\left[\frac{(1-z_\sigma)^2}{\alpha_\sigma' z_\sigma}\right] + \frac{1+z_\sigma}{1-z_\sigma} \tag{21}$$

and $\xi_\sigma' \equiv \partial \xi_\sigma / \partial d$. One should note in the following discussion that:

$$\begin{aligned} &g(z_\sigma) > 0, \quad z_\sigma > z_\sigma^m \\ &g(z_\sigma) \le 0, \quad z_\sigma \le z_\sigma^m \, , \end{aligned} \tag{22}$$

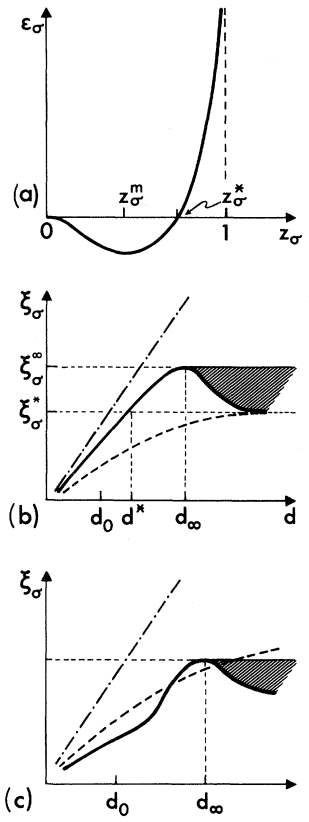

FIG. 2. (a) Schematic plot of $\epsilon_\sigma(z_\sigma)$, defined in Eq. (16). The quantity z_σ^* moves to the right for decreasing α_σ and to the left for increasing α_σ. The parameter α_σ is introduced in Eq. (13). (b) Schematic plot of the reduced melting temperature ξ_σ as a function of crystal thickness d for $\partial f_\sigma / \partial d < 0$. The dashed-dotted curve shows the behavior without screening, whereas the solid and dashed curves are typical for weakly and strongly screened dislocation pairs, respectively. The indices $(*, \infty, 0)$ are explained in the text. (c) Schematic plot of ξ_σ vs d for $\partial f_\sigma / \partial d > 0$. The dashed-dotted and solid curves illustrate the behavior for no and weak screening, respectively, where it has been assumed that $f_\sigma(\xi_\sigma, \infty) = 0$. The dashed curve shows the strongly screened case with $f_\sigma(\xi_\sigma, \infty) < 0$.

where the z_σ^m denotes the minimum of $\epsilon_\sigma(z_\sigma)$ [see Fig. 2(a)]. If $\partial f_\sigma / \partial d < 0$ in Eq. (20) one obtains

$$\xi_\sigma'(z_\sigma^m) \equiv \left|\frac{\partial f_\sigma}{\partial d}\right| \Big/ \frac{\partial f_\sigma}{\partial \xi_\sigma} < 0 \, . \tag{23}$$

From Eqs. (19)–(23) it follows that in the domain $\xi_\sigma' > 0$, $\xi_\sigma' < \xi_\sigma / d$ for $z_\sigma > z_\sigma^m$, and that $\xi_\sigma' < 0$ for $z_\sigma < z_\sigma^m$. Furthermore, since $z_\sigma \to 0$ when $d \to \infty$ it follows that $f_\sigma(\xi_\sigma(\infty), \infty) + \gamma_\sigma = 0$.

The qualitative behavior of the reduced melting temperature ξ_σ as a function of layer thickness d is illustrated in Fig. 2(b). The physical situation of

weak-pair screening with $\alpha' > 0$ is shown as the bold solid curve. The unscreened curve $\alpha' = 0$ shows a linear dependence on d, whereas the case of strong screening is given by the dashed curve.

For the physical case, the linear behavior was lost for $d > d_0$, as discussed earlier. The quantity d^* is obtained as the solution to $\epsilon_\sigma \equiv 0$, whereas d_∞ denotes the value at which ξ_σ takes a maximum. For $d > d_\infty$, the d dependence of the screening of the elastic interaction in our model becomes so strong as to increase the stability of the liquid state over that at d_∞. In Sec. IV, however, we argue that the effective thickness of a layer decreases with increasing temperature. As will be discussed there, this leads to freezing at d_∞, and offers a tentative explanation of a possible polymer folding instability for ultralong polymer chains that are grown from the melt. We indicate these regions of possible instability with cross hatching in Figs. 2(b) and 2(c). Although paraffins of sufficient length have not been attained in the laboratory, the possibility of observing this instability is intriguing.

The behavior of ξ_σ vs d for $\partial f_\sigma / \partial d > 0$ is shown in Fig. 2(c). From Eq. (20) one obtains

$$\xi'_\sigma(z_\sigma^m) \equiv -\frac{\partial f_\sigma}{\partial d} \Big/ \frac{\partial f_\sigma}{\partial \xi_\sigma} > 0 \tag{24a}$$

and $\xi'_\sigma \geq 0$ for $z_\sigma \geq z_\sigma^m$. Furthermore, the following inequalities must hold. For $\xi'_\sigma \lessgtr \xi_\sigma / d$

$$\frac{\partial f_\sigma}{\partial d} \Big/ \frac{\partial f_\sigma}{\partial \xi_\sigma} \lessgtr \xi'_\sigma \tag{24b}$$

and for $\xi'_\sigma \gtrless \xi_\sigma / d$

$$\frac{\partial f_\sigma}{\partial d} \Big/ \left| \frac{\partial f_\sigma}{\partial \xi_\sigma} \right| \gtrless \xi'_\sigma \,, \tag{24c}$$

for $z_\sigma \gtrless z_\sigma^m$, respectively. These latter equations are not very restrictive for the behavior of $\xi_\sigma(d)$, but obviously Eq. (24c) fails for $d \to \infty$, since $\xi'_\sigma > \xi_\sigma / d$, preventing z_σ from vanishing. In Fig. 2(c) two possible screened-case behaviors are indicated, although an exact discussion requires a knowledge of $f_\sigma(\xi_\sigma, d)$.

According to Fig. 2(a), $\epsilon_\sigma \leq 0$ in the region $0 \leq z_\sigma \leq z_\sigma^*$, and from Fig. 2(b) for the physical case (bold line), this corresponds to $d \gtrsim d^*$. However, this does not necessarily indicate an instability in the system for $\xi_\sigma > \xi_\sigma^*$, since the elastic interaction energy of the pairs is not included in ϵ_σ. Furthermore, Eq. (15), which is based on the ideal gas approximation, may fail in this regime. One sees that for $z_\sigma \leq z_\sigma^*$, $n_\sigma \langle r_\sigma^2 \rangle_0$ may approach the order of 1, so that bound pairs may considerably overlap. It is also in this regime that Eq. (13) is not at all well approximated by Eq. (13'). In fact the overlap of bound pairs may already occur for $d < d_0$. This point may partially be remedied through the introduction of a Van der Waal's approximation for the gas of bound pairs.[6]

A typical edge dislocation bridge, as we have defined in Sec. I, has small portions which run parallel to the lamellar plane of screw character. These segments are formed in the polymer crystal by aggregates of kinks.[3] This induces substantial pulling and dragging of the molecules as a whole. In a proper treatment of the problem the free energy associated with this effect, as well as that of the core energy of the kinked dislocation segments, must be included in $f_\sigma(\xi_\sigma, d)$. Furthermore, the elastic interaction arising from the kinked segments must be included in f_σ as well. These contributions will remain small only as long as the essentially *straight* bridging character of the dislocations is preserved near the melting point. This is only possible if d is small enough to maintain the essentially two-dimensional character of the problem.

In fact, if the kinked segments appear essentially in pairs of opposite sense along the dislocation bridge, then their long-range interaction is essentially screened out, so that the following approximation may be made for large d:

$$f_\sigma(\xi_\sigma, d) \approx f_\sigma(\xi_\sigma, \infty) + O(1/d) \,, \tag{25}$$

where the last term is due to surface effects. In this case ξ_σ^∞, as indicated in Fig. 2(b), will be essentially given by $z_\sigma^\infty d_\infty \approx z_\sigma^m d_\infty$. If we expand Eq. (16) about the maximum of ξ_σ we obtain

$$(\xi_\sigma - \xi_\sigma^\infty) \approx -\frac{1}{2} \left| \frac{\partial f_\sigma}{\partial \xi_\sigma} \right|_{\xi_\sigma^\infty} \left[\frac{z_\sigma^\infty (2 - z_\sigma^\infty)}{(1 - z_\sigma^\infty)^2} \right] \times \left[\frac{d - d_\infty}{d_\infty} \right]^2 . \tag{26}$$

This formula can easily be fitted to the experimental curve, given in Fig. 1 between $n = 40$ and 110 for the weakly screened case [bold curve in Fig. 2(b)], if we assume that $n = 110$ corresponds to d_∞. For $n < 40$, the experimental curve bends more strongly downward than Eq. (26) suggests, indicating that further terms in the Taylor series are needed.

A calculation of $f_\sigma(\xi_d, d)$, using matrix methods developed by DiMarzio and Rubin,[13] is currently being carried out by one of us, and will be published elsewhere.[14] There, the relative importance of bridging versus nonbridging dislocations to the behavior of $T_m(d)$ is being estimated, as well as the

contribution due to bridges which wander largely in a direction perpendicular to the polymer chain axis.

It should be emphasized perhaps at this point that the long-range interactions are of an elastic nature and due to steric constraints. For $\partial f_\sigma/\partial d > 0$, because of the thermodynamic relations, Eq. (19), one may be lead to consider the following large d behavior of $f_\sigma(\xi_\sigma, d)$

$$f_\sigma(\xi_d, d) \simeq -\xi_\sigma^x d^{y-1} , \tag{27}$$

where the constants $y < 1$ and $x > 0$. In this case ξ_σ vs d behaves as shown in Fig. 2(c) (dashed curve). Equation (27) implies a linear dependence of ξ_σ on d for large d, a dependence which is not observed experimentally. This fact leads us to suspect that a different type of instability occurs for large d crystals which are grown from the melt.

As mentioned earlier, the kink conformations of the polymers tend to drag and push along their main axis as a whole. Supposing that Eq. (25) is invalidated by Eq. (27) for very large d (for example $d > d_\infty$), then the long-range elastic energy due to kinking may be considerably reduced in a folded polymer structure. In that case only that part of the molecule corresponding to the folding period must be dragged or pushed when the kink portions of the dislocation bridge are generated or annihilated. Because the average end-to-end length d_{eff} of the polymers in the melt is rather small compared to their extended length, they will not be able to fluctuate into their extended form when entering the hatched regions of Fig. 2 for fixed d and decreasing ξ_σ, but in fact will solidify at the temperature ξ_{eff}, corresponding to d_{eff}. This discussion lends further support to the possibility of a folding transition for d somewhat larger than that attained at present for n-paraffin crystals.

III. ROTATOR PHASE

Due to the planar zig-zag structure of the polymer chains,[9] the molecules, viewed in cross section (i.e., in a plane perpendicular to the chain axis), have an orientation, which we may denote with a planar vector. At the lowest temperatures the crystal structure is orthorhombic,[9] and the orientation of the molecules is as shown in Fig. 3(a). In this figure a pair of defects in the structure is also indicated, and it is obvious that this aspect of the system may be described by an anisotropic rotator model on a compressible lattice. At a temperature T_r near and below T_m these rotators become disordered in the lamellar plane,[9] a state which we term "the rotator phase." The crystal structure in this phase is hcp.[9] A study of the transition at T_r which parallels that given in Sec. II for T_m may be carried out, in which vortex pairs play the role of dislocation point defects. For this case we expect a discontinuous transition, due to the compressibility of the lattice.

Instead of pursuing this point further, we will concern ourselves in this section with the structural properties of the rotator phase. In the low-temperature phase the rotational degrees of freedom are essentially discrete, whereas in the more loosely packed hexagonal phase the rotators should move more freely. The defects in the anisotropic rotator model are domain walls and vortices.[15] A pair of point vortices of opposite strength is indicated in Fig. 3(b) by $(+,-)$ for a simple monolayer. The spins on opposite sides of the dashed line are rotated by $\pm\pi$ as indicated by the dashed arrows in the

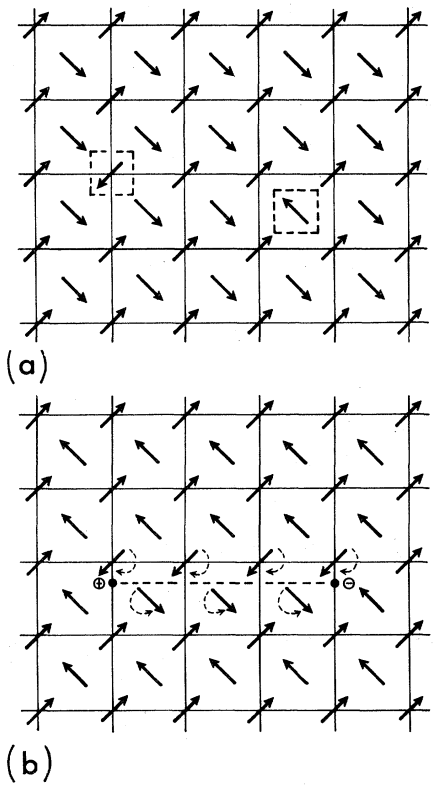

FIG. 3. (a) Zig-zag plane orientation of polymer molecules in the orthorhombic structural phase of paraffin. Arrows indicate this orientation as viewed from the surface of the lamella. Two single polymer orientational defects are also shown in the dashed boxes. (b) Pair of point vortices $(+,-)$ in a hypothetical paraffin monolayer at low temperatures. The spins above and below the dashed line are rotated through $\pm\pi$ as indicated by the dashed curved arrows.

figure. This line may be thought of as a cut in the planar crystal, where rotator couplings on opposite sides are broken and then reestablished after the rotations are carried out.

For a lamella of finite thickness d, the dashed line corresponds to one boundary of a cut surface, as illustrated in Fig. 4(a). This cut surface is a plane whose normal lies parallel to the lamellar surface, its border being a vortex loop which begins at $(+)$ and ends at $(-)$ on the upper lamellar surface. The polymers to either side of this surface are twisted through $+\pi$ and $-\pi$, respectively. The twist is indicated as being rather localized at a distance l_0 below the lamellar surface at a depth at which the vortex line runs parallel to it. In Fig. 4(a) the polymers shown are on one side of the cut surface, and are represented as structures of an elliptical cross section of major axis r_p. The arrows at either end of the polymers indicate the orientation of the zig-zag planes.

If such a vortex loop touches the opposite lamellar surface, two vortex lines of opposite strength are created. The dissociation of such pairs can be treated analogously in discussing the rotator phase transition at T_r, as was done in Sec. II for T_m. The convex shape of $T_r(d)$ is a consequence then of the entropy generating configurations of such vortex bridges.

We now consider the *motion* of vortex loops of the type illustrated in Fig. 4(a), which may occur thermally or in response to external stresses. In a *static* situation the energetically most favorable situation is such that the cut surface is planar with normal in the lamellar plane. The geometrical reason for this becomes obvious if one considers a planar vortex loop, whose cut surface is *parallel* to the lamellar plane. Then, of necessity, all polymer molecules piercing through this cut surface are twisted by a full revolution, clearly an energetically unfavorable situation. This problem does not arise for the usual planar rotator model, and is a feature imposed by the connectivity constraint on the polymer molecules.

In a *dynamic* situation a *macroscopic* vortex loop cannot move as a whole in a direction perpendicular to its cut plane in discrete hops of one-lattice spacing. This would require that the loop overcome a macroscopically large energy barrier proportional to the loop's interaction energy. Accordingly, the vertical portions of the vortex loop develop kink segments, which slide down along the chain axis direction, as illustrated in Fig. 4(b). Finally, a pair of bridging vortices of opposite strength result, which are displaced one-lattice spacing from the original position of the loop in a direction perpendicular to it.

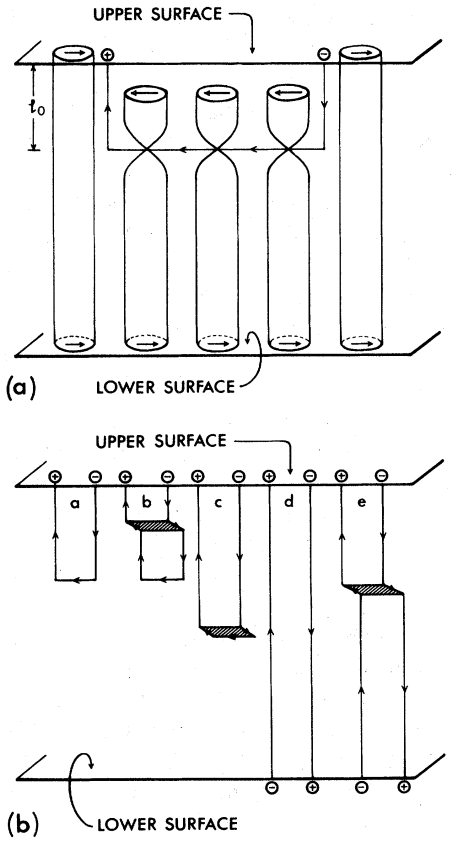

FIG. 4. (a) Vortex loop in a polymer lamella. Polymers are indicated as structures of elliptical cross section, whose major axes indicate the orientation of the zig-zag planes (arrows at the polymer ends). The polymers shown, lie to one side of the plane of the vortex loop, those to the other side of this plane (not shown) are twisted in the opposite sense by the same amount. The situation as viewed from the upper lamellar surface would appear as in Fig. 3(b). (b) Motion of a macroscopic vortex loop perpendicular to its cut surface. The loop develops parallel kink segments in the direction of motion (oblique to the figure surface) $(a)\rightarrow(b)$, which slip downward along the direction of the polymer axis $(b)\rightarrow(c)$, until the loop has moved one-lattice spacing in a direction normal to its cut plane (into the figure plane) (d). In the step $(c)\rightarrow(d)$ the hatched surface, which lies parallel to the lamellar surface moves to the lower surface, creating a pair of bridging vortices. This pair continues to move through the development of further parallel kink steps $(d)\rightarrow(e)$.

As is apparent from the figure, a small hatched step in the cut surface appears during the motion with the energetically unfavorable orientation (i.e., parallel to the lamellar surfaces). The hatched step

then proceeds to move downward until it disappears at the lower lamellar surface. The resulting bridging vortex pair continues to move through further kink pair formation near the upper lamellar surface, and subsequent sliding of the resulting step to the lower surface.

As the cut surface of a bridging vortex loop approaches a given polymer from infinity, this polymer *rotates* about its axis through $+\pi$ with respect to its original orientation, before which it pierces the step in the cut surface. Then, that portion of the polymer above the step *twists* through $+\pi$ about its axis, whereas that portion below *twists* through $-\pi$. Clearly, the twisted region of the polymer, which is localized near the step, slides from the top lamellar surface to the bottom, as the cut surface of the vortex pair undergoes a displacement of one-lattice spacing in the direction of its normal. Since these 2π twists appear first at the upper lamellar surface, the polymers, piercing the step, contract by a length r_p at their upper ends, r_p characterizing the polymer's cross section. As is shown in Fig. 5, the twisted section slips to the lower end of the polymer during the vertical motion of the step, "drilling" it into the neighboring lamella a distance of order r_p.

Thus, the motion of a bridging pair in the direction of the normal to its cut surface sweeps out a depressed area on one lamellar surface, and a corresponding raised area on the other. In this way a pair of straight steps is traced out on each lamellar surface.

It should be noted that if the cut surface of the bridging pair moves *parallel* to its plane, kink motions of the vertical segments do not involve the energetically unfavorable intermediate-step areas [hatched areas in Fig. 4(b)]. Such motion will be termed "cross slip" in analogy with dislocation-loop terminology. Obviously, the polymers involved in this motion are only rotated through $\pm\pi$ on either side of the moving loop, and the drilling effect, and corresponding distortions of the lamellar surfaces are absent.

Thus in an *arbitrary* vortex pair trajectory, pairs of surface step *segments* should appear. The end points of these surface step segments may be associated with the points at which screw dislocations, with Burgers vectors $\pm\vec{b}_s$ along the polymer axis direction, pierce the lamellar surfaces, if the following condition is met:

$$b_s = 2\pi m r_p \ , \tag{28}$$

where m is some integer. We expect these conditions on the lattice displacements to be favorable for steric reasons. Since each pair of screw dislocations

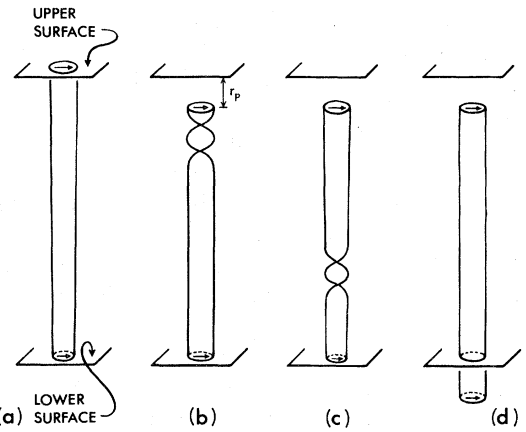

FIG. 5. Twisting and drilling motion of a single polymer, due to its passage through the cut plane of a bridging vortex pair. The 2π twist is assumed to be rather localized in the sliding step of the cut plane of the bridging vortex pair [hatched area of Fig. 4(b)].

tends to annihilate in order to reduce the crystal strain, the motion of the vortex pair in the direction along the normal to its cut surface will be impeded, perhaps prohibitively.

Thus we conclude from the above discussions that the random motion of vortex loops, generated by thermal fluctuations, *could* lead to a roughening of the lamellar surfaces, or even to a complete destruction of the lamellate ordering, without destroying the lateral hexagonal order. The degree and very nature of this type of disordering depends upon the detailed coupling mechanism between moving vortices and screw dislocations. This problem is currently being studied.

Finally it should be noted that, even in the absence of the rotator phase and the presence of moving vortex pairs, the edge dislocations of Sec. II will considerably roughen the lamellar surfaces in the thicker lamellates near T_M. In the static case of thermal production of edge pairs with lateral screw segments, shortening of those polymers contained in the cut plane of the randomly produced pairs will lead to surface roughening. This static edge pair roughening disappears for $d < d_0$ (see Sec. II) however, since in this region the polymers may be considered quite stiff, so that no lateral screw segments, which are necessary for polymer shortening, can form.

Furthermore, for $d < d_0$ the cross-slip motion of the edge pairs may proceed through the vertical sliding of steps in a manner similar to that described in Fig. 4(b) for vortex pairs. In this case the step sliding may be viewed as a kink in those polymers which pierce the step, the vertical sliding

of the kink pulling the polymers along their axes out of the lamellate without rotation, a distance of the order of one-lattice spacing. Thus the cross-slip motion of edge pairs also leads to the appearance of surface-step segments, whose end points are the points at which a pair of bridging screw dislocations pierce the lamellar surface. Thus we expect a certain degree of surface roughening even when an intermediate rotator phase is absent for $d > d_0$.

IV. ORDERING IN THE PARAFFIN MELT

So far we have considered three defect types which may be operative in the melting of paraffin. The dissociation of bridging vortex pairs may destroy the orthorhombic orientation of the polymer zig-zag planes, precipitating the rotator phase. The dissociation of bridging edge dislocations may destroy the lateral hexagonal order of the rotator phase, and the dissociation of screw dislocation pairs may destroy the lamellate ordering. Considering only these effects one would predict a nematic state for the melt. Here we wish to argue that the motion of edge dislocations may destroy the *axial order* of the paraffin chains, as well as the lamellate structure which we described in Sec. III, so that the dissociation of the bridging screw dislocations associated with their motion (see end of Sec. III) can destroy the axial and lamellate order simultaneously for $d > d_0$.

It is well known that nonconservative dislocation motion in normal crystals proceeds by absorption and emission of vacancies which diffuse into the crystal from the surface, the energy of formation for an interstitial-vacancy pair in the bulk being extremely high. The diffusion into the bulk of a *polymer* vacancy, produced near a free surface of the crystal, is illustrated in Fig. 6. Here the vacancy is shown as a dashed line, and the polymers near the free surface as solid lines in Fig. 6(a). Through polymer jogging the vacancy becomes increasingly partitioned [Figs. 6(b)–6(d)], so that in thermal equilibrium a distribution of vacancy *segments* are available in the bulk to initiate nonconservative motion of dislocation loops. Thus an initially planar-edge dislocation bridge of the type discussed in Sec. II will absorb and emit vacancy segments during nonconservative climb processes, becoming three dimensional in nature. We therefore expect that the nonconservative edge motions will enhance the production of lateral segments in bridging edge dislocations for $d > d_0$. These additional dislocation segments lead to polymer conformations out of

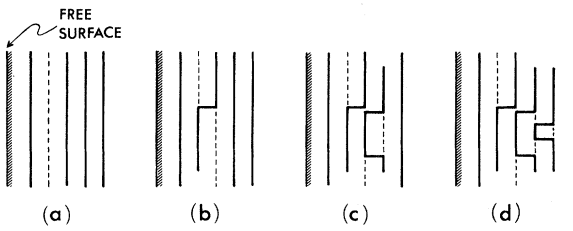

FIG. 6. Formation process of a partitioned polymer vacancy, created near a free surface, through the mechanism of polymer jogging.

the original slip plane of an edge pair. Thus, we expect an increased predominance of polymer conformations with a substantial *lateral* component. This increased deviation from axial order of the polymers can be enhanced by the *intersection* of edge dislocations with the lateral polymer segments as shown in Fig. 7. Here the slip plane of a straight bridging edge dislocation (dashed line) is taken to be the figure plane; whereas the plane of the conformed polymer (solid line) is taken to intersect this slip plane at an angle of $\pi/3$. This is usually the case for the hexagonal structure, when the polymer under consideration is not involved in nonconservative dislocation motion. (In that case it would not lie on a plane, but the general conclusions of the case shown in Fig. 7 would still be valid.) The arrows in Fig. 7 indicate the forces on the polymer, due to the slip constraint, imposed by the presence of the dislocation. We see that the polymer is stretched laterally by such encounters.

It should be emphasized that the jogged portions of the polymer are participating in lateral screw segments of edge dislocations, so that the encounter shown in Fig. 7 actually represents the intersection

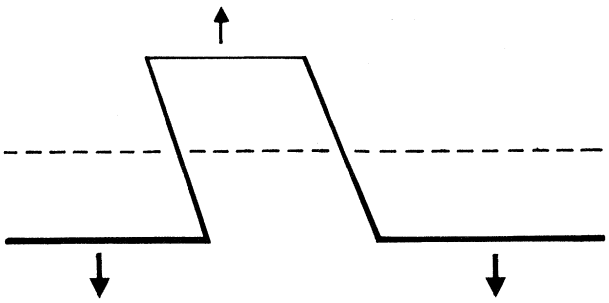

FIG. 7. Intersection of a conformed polymer (solid line) with a straight bridging edge dislocation (dashed line). The slip plane of the dislocation is that of the figure, whereas the plane of the conformed polymer cuts the figure plane at an angle of $\pi/3$. Arrows indicate the direction of force on the polymer, due to the slip constraint imposed by the presence of the dislocation.

of two edge dislocations (at least) in different allowed slip planes of the hexagonal structure. From Fig. 7 we see that such processes involve a lateral dragging of the polymer molecules, and we suspect that they will be an important factor in the destruction of nematic order near T_M for lamellates in which polymer kinking is possible in the solid state ($d > d_0$).

V. DISCUSSION

In Sec. II of this paper we have developed a melting theory of paraffin crystals, based on the dissociation of screened bridging edge dislocations in a lamellate of thickness d. Although the theory gives a qualitatively correct description of $T_M(d)$, no quantitative comparison has been possible, due to our incomplete knowledge of $f_\sigma(\xi_\sigma, d)$. Furthermore, our restriction to treating only nearly straight bridging edge pairs is a severe one. And as we have seen in Sec. III, a proper melting theory must include the detailed structure of the rotator phase.

In fact, the vortex-motion surface roughening in the rotator phase may be so strong as to destroy the lamellate, leaving only axial and hexagonal lateral order with a longitudinal-correlation length λ_d (along the polymer axis), which must replace the length d in the melting theory of Sec. II. A more severe surface roughening may produce liquidlike properties longitudinal to the polymer axis already within the rotator phase.

The melting theory of Sec. II predicts a maximum in $T_M(d)$ at d_∞, which has not been observed experimentally. We believe that this maximum is not an artifact of our approximations, but rather that a folding instability of the polymer experimentally occurs at d_∞.

In our discussion of the defects associated with the rotator transition in Sec. III, we considered only those of the vortex loop type, although *domain walls* may also be present near T_r. Obviously domain walls which run parallel to the lamellar surfaces must involve polymer twisting across their boundaries, due to the connectivity of the polymers. We expect such twisted *layers* to be highly unfavorable energetically. The walls which exist perpendicular to the lamella, and which bridge it, will lead inevitably to $T_r \sim d$ for reasons similar to those given in Sec. II for the dissociation of *straight* bridging edge dislocation pairs, leading to $T_M \sim d$. Since the entropy associated with the energetically unfavorable configurations of the domain walls with large flat regions parallel to the lamellar surface are needed to explain the bending over of $T_r(d)$ for $d > d_0$, we believe that domain-wall defects play only a minor role in the precipitation of the rotator phase.

Finally in Secs. III and IV we discuss the effect of vortex pairs and dislocation lines on the layered structure, which we imposed on our calculation in Sec. II. There we have argued that cross-slip motion of vortex pairs in the rotator phase may lead to a "drilling" of polymers along their axes, out of the lamellate, to which they initially belong, leading to surface roughening. Also we have shown that the motion of edge pairs may cause surface roughening through a similar mechanism, and that intersection of such defects, lying in different slip planes, may lead to a complete destruction of nematic order in the melt.

ACKNOWLEDGMENTS

We gratefully acknowledge stimulating discussions with Professor H. Gleiter, Professor M. Zuckermann, and Dr. J. Krüger. This work was supported by Deutsche Forschungsgemeinschaft within Sonderforschungsbereich 130—Ferroelektrika.

[1]M. G. Broadhurst, J. Chem. Phys. 36, 2578 (1962).
[2]P. J. Flory and A. Vrij, J. Am. Chem. Soc. 85, 3548 (1963).
[3]John Doe, *Macromolecular Physics, Polymer Melting,* edited by B. Wunderlich (Academic, New York, 1980), Vol. 3.
[4]D. Kuhlmann-Wilsdorf, Phys. Rev. 140, 1599 (1965).
[5]J. M. Kosterlitz and D. J. Thouless, J. Phys. C 6, 1181 (1973).
[6]A. Holz and J. F. N. Medeiros, Phys. Rev. B 17, 1161 (1978).
[7]B. A. Hubermann, D. M. Lublin, and S. Doniach, Solid State Commun. 17, 485 (1975).
[8]G.-R. Strobl, Phys. Bl. 33, 550 (1977); W. Pechhold, Kolloid Z. Z. Polym. 228, 1 (1968).
[9]J. Krüger (private communication).
[10]A. Holz, Phys. Rev. A 20, 2521 (1979); Physica (Utrecht) 109A, 58 (1981).
[11]A. Holz, Physica (Utrecht) 111A, 217 (1982).
[12]A. Holz, presented at NATO Conference on Two-Dimensional Physics, Erice, Sicily, 1979 (unpublished).
[13]E. A. DiMarzio and R. J. Rubin, J. Chem. Phys. 55, 4318 (1971).
[14]D. T. Vigren (unpublished).
[15]A. Holz, Physica (Utrecht) 97A, 75 (1979).